Proton Magnetic Resonance Characterization of Phoratoxins and Homologous Proteins Related to Crambin†

Juliette T. J. Lecomte,‡,§ David Kaplan,‡ Miguel Llinás,*,‡ Eva Thunberg,∥ and Gunnar Samuelsson∥

Department of Chemistry, Carnegie-Mellon University, Pittsburgh, Pennsylvania 15213, and Department of Pharmacognosy, Biomedical Center, University of Uppsala, S-751 23 Uppsala, Sweden

Received July 28, 1986; Revised Manuscript Received September 16, 1986

ABSTRACT: The mistletoe protein toxins ligatoxin, phoratoxins A and B, and viscotoxins A3 and B have been investigated by ^{1}H NMR spectroscopy at 300 and 600 MHz. The five polypeptides define a set of closely related homologues, containing 46 amino acid residues each, in a structure constrained by three cystine bridges. Their methyl and aromatic spectra were analyzed and a number of signals identified and assigned via comparative criteria, two-dimensional chemical-shift correlated spectroscopy, acid–base titration, and proton Overhauser experiments in ^1H_2O. The spectra indicate a compact globular conformation and a common folding pattern for the toxins. In particular, use was made of well-resolved aliphatic and aromatic resonances in order to compare the mistletoe proteins with the thionins, a set of homologous toxins from gramineae, and with crambin, a closely related polypeptide from a crucifer, which we have previously studied by NMR. We observe that while all the investigated proteins have very similar secondary and tertiary structures, they differ widely in their dynamic characteristics as probed by the amide N*H* ^{1}H–^{2}H exchange kinetics in deuteriated solvents; thus, while crambin and the thionins exhibit very fast isotope exchange, the kinetics for the mistletoe toxins are slow, with some N*H* groups showing exchange half-lives that extend up to several days at pH* 5.8 or that are too long to be measurable at ambient temperature. The temperature dependence of the ^{1}H NMR spectrum also indicates that the toxins are endowed with a thermally very stable native (ground-state) structure, with little evidence of large amplitude structural breathings up to ~370 K, although irreversible chemical degradation (denaturation) becomes evident at temperatures ≳350 K. It is concluded that the mistletoe toxins afford valuable rigid structures for NMR conformational studies.

The European mistletoe (*Viscum album* L.), a member of the *Loranthaceae* family, has been used for centuries in medicine. In the early 1900s, its power against neoplastic diseases was tested, and the investigations resulted in the commercialization of leaf and stem extracts (Selawry et al., 1961). The material from *Viscum album* L. contains at least five polypeptides exhibiting various degrees of cytotoxicity (Konopa et al., 1980) and cardiotoxicity (Rosell & Samuelsson, 1966). The five proteins identified among the *Loranthaceae* (Winterfeld & Bijl, 1948; Samuelsson, 1961, 1966; Samuelsson & Ekblad, 1967) present a high degree of homology with crambin (Van Etten et al., 1965; Teeter et al., 1981) and the thionins (Redman & Fisher, 1969; Jones et al., 1982). They are known as viscotoxins. Viscotoxins A2, A3, and B are the main components and have been sequenced (Samuelsson et al., 1968; Samuelsson & Pettersson, 1971a; Olson & Samuelsson, 1972). Biologically active viscotoxin A3 interacts with DNA whose thermal denaturation it retards (Woynarowski & Konopa, 1980); the in vivo relevance of the phenomenon has not been investigated yet. The American mistletoes (*Phoradendron*) produce parent toxins called phoratoxins or ligatoxin (Samuelsson & Ekblad, 1967; Mellstrand & Samuelsson, 1973; Mellstrand, 1974; Thunberg & Samuelsson, 1982a). Two variants of phoratoxins are known, the A and B, which have been sequenced (Mellstrand & Samuelsson, 1974a; Thunberg, 1983). The primary structure of ligatoxin A has also been determined (Thunberg & Samuelsson, 1982b).

The mistletoe toxins are basic polypeptides (p*I* > 11.5) composed of a single chain of 46 amino acid residues constrained by three disulfide bonds (Samuelsson & Petterson, 1971b; Mellstrand & Samuelsson, 1974b) contributing to their thermal stability (Samuelsson & Pettersson, 1971b; Woynarowski & Konopa, 1980). Their primary structures are presented in Figure 1A, which also includes that of crambin. The toxicity has been compared to that of proteins extracted from snake venoms (Konopa et al., 1980).

Elsewhere we have reported on the ^{1}H NMR[1] spectral characteristics of crambin (Llinás et al., 1980; De Marco et al., 1981; Lecomte et al., 1982a; Lecomte & Llinás, 1984a,b) and the thionins (Lecomte et al., 1982b). The sequence homology relating crambin and the thionins to the mistletoe toxins prompted us to investigate five of the latter: ligatoxin A, phoratoxins A and B, and viscotoxins A3 and B. From an NMR spectroscopic standpoint, this set of homologues is expected to be informative for assigning resonances and understanding the structure of crambin-related proteins as they exhibit a range of amino acid compositions complementary, in some respects, to those of crambin and the thionins. For example (Figure 1B), ligatoxin A and the two phoratoxins contain alanine at sites 9 and 27, a feature that is common

†This research was supported by the U.S. Public Health Service, NIH Grants GM-25213 and HL-29409. The 600-MHz NMR facility is supported by Grant RR 00292 from the National Institutes of Health.

‡Carnegie-Mellon University.

§Present address: Department of Chemistry, University of California, Davis, CA 95616.

∥University of Uppsala.

[1] Abbreviations: CD, circular dichroism; NOE, nuclear Overhauser effect; pH*, glass electrode pH reading uncorrected for deuterium isotope effect; pK_a*, pK_a determined in ^2H_2O (uncorrected for deuterium isotope effect); NMR, nuclear magnetic resonance; SECSY, two-dimensional spin-echo correlated spectroscopy; 2-D, two dimensional.

0006-2960/87/0426-1187$01.50/0

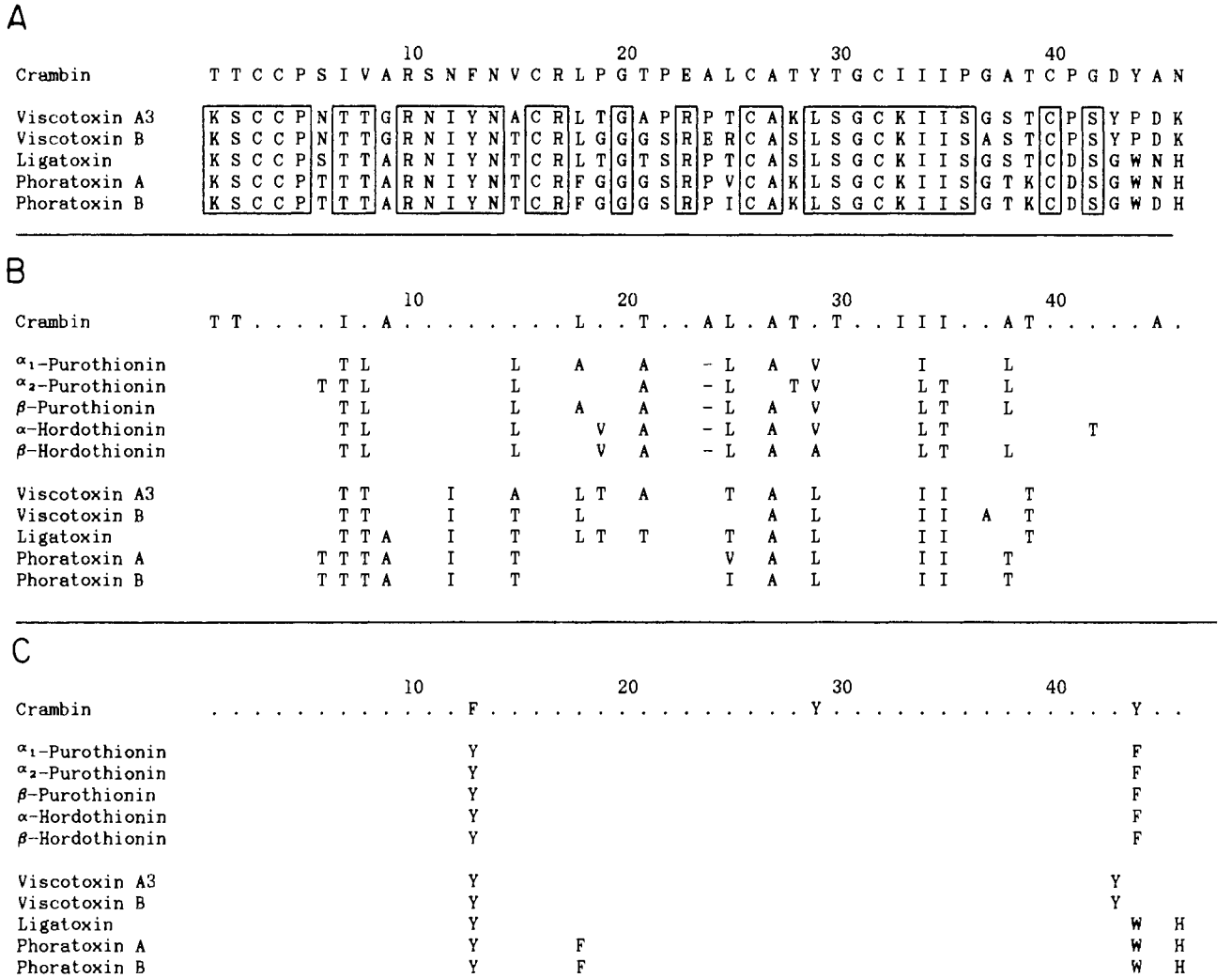

FIGURE 1: Amino acid sequences of mistletoe toxin homologues: (A) comparison of the primary structure of the homologues studied in this project; (B) methyl-containing residues; (C) aromatic residues. Homologues sections of the mistletoe proteins' sequences are framed.

with crambin, while the latter also contains this residue at sites 24, 38, and 45. On the other hand, Ala residues are also found at sites 21 (viscotoxin A3) and 37 (viscotoxin B), which unambiguously identifies the corresponding resonances. Equally interesting is the aromatic makeup of the mistletoe toxins: phoratoxins A and B contain one of each of the four aromatic residues (His, Phe, Tyr, and Trp). In particular, the presence of Phe and His residues at sites 18 and 46, respectively, is unique among the mistletoe toxins as their homologues most often fill these positions with aliphatic residues. Also novel is the presence of a Trp residue at site 44, known in crambin to be somewhat constrained by the tertiary folding (Hendrickson & Teeter, 1981; De Marco et al., 1981; Lecomte & Llinás, 1984a,b). It should be stressed that aromatic side chains afford valuable NMR reporter groups in protein conformational studies: they often yield well-resolved and characteristic signals while perturbing resonances arising from neighbor groups through anisotropic ring-current effects.

The positions of the aromatic and methyl-containing residues for crambin and the five related thionins studied in this project are given in Figure 1 (parts C and B, respectively). Our attempts to uncover correspondences among their proton spectra concentrated on signals arising from these residues. Furthermore, in this paper we have investigated the $^1H-^2H$ exchange of the amide N*H* groups in ^2H_2O. We find that the isotope exchange is much slower for the mistletoe toxins than for the thionins. This suggests that the two sets of proteins are dynamically different, the toxins being less flexible. This is unexpected considering the additional disulfide bridge found in the thionins.

Materials and Methods

Viscotoxins A3 and B were isolated from leaves of *Viscum album* L. (Samuelsson & Petterson, 1970). Ligatoxin A was obtained from leaves and stems of *Phoradendron liga* (Gill.) Eichl. (Thunberg & Samuelsson, 1982a). Phoratoxin A was isolated from leaves of *Phoradendron tomentosum* (DC) Englem. subsp. *macrophyllum* (Cockerell) Wiens, grown on *Juglans hindsii* (Mellstrand & Samuelsson, 1973). Phoratoxin B was obtained from the same mistletoe species but growing on *Populus fremontii* (Thunberg, 1983). All mistletoe toxins were of the same batches that had previously been used for determination of their amino acid sequences (Samuelsson et al., 1968; Samuelsson & Petterson, 1971a; Olson & Samuelsson, 1972; Mellstrand & Samuelsson, 1974a; Thunberg, 1983). They were homogeneous in ion-exchange chromatography experiments and on polyacrylamide gel electrophoresis. The amino acid analyses integrated satisfactorily.

For the NMR studies, samples of the various proteins were dissolved in ^2H_2O to a concentration of ~1–2 mM. After the pH* was adjusted, typically to 6.25, the ^1H NMR spectra were recorded in the Fourier mode at 300 MHz or at 600 MHz on a Bruker WM-300 spectrometer or at the NIH National NMR Facility for Biomedical Studies at Carnegie-Mellon

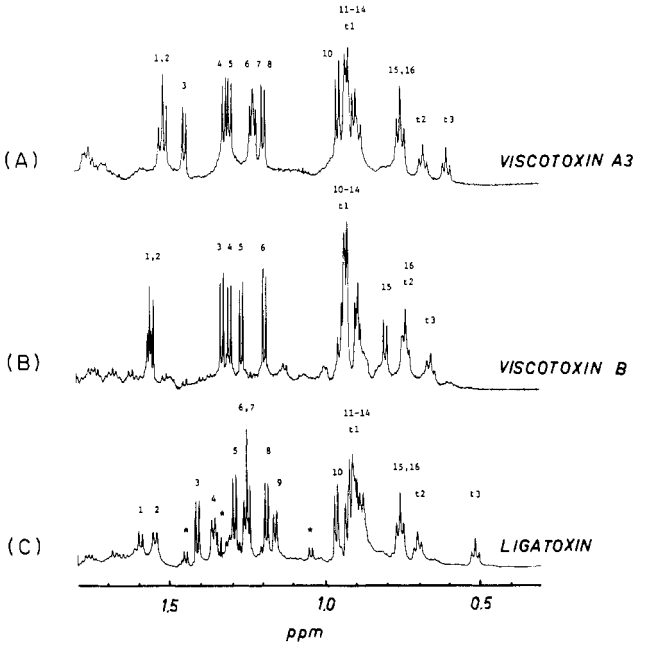

FIGURE 2: ^{1}H NMR spectrum of mistletoe toxin homologues at 600 MHz, methyl region. Solvent: ^2H_2O, pH* 6.3, 298 K. (A) Viscotoxin A3, (B) viscotoxin B, and (C) ligatoxin. Signals are numbered from low to high field; the asterisk (*) indicates impurities. Except for isoleucyl CH_3^δ triplets (t), all resonances are doublets.

University, respectively. Two-dimensional spin-echo correlated (SECSY) experiments (Aue et al., 1976) were implemented according to Nagayama et al. (1979). The digital resolution in both dimensions was 5 Hz. Dioxane was used as an internal reference; chemical shifts are referred to the sodium 3-(trimethylsilyl)[2,2,3,3-$^2H_4$]propionate signal, assumed to resonate at −3.766 ppm from dioxane (De Marco, 1977). The temperature of the NMR probe was determined with a methanol sample (Van Geet, 1972). Homonuclear spin–spin decoupling was applied systematically to all the solutions, and the data were analyzed taking into account the vicinal spin-coupling values ^3J (Lecomte et al., 1982a,b). The temperature and pH* of the phoratoxin samples were varied when the aromatic region was investigated. For the experiments in water, suppression of the strong ^1H_2O signal was achieved via long pulse excitation (Redfield, 1978), with pulse width 380 μs, giving a flip angle of ~36°.

Results and Discussion

Analysis of Methyl Resonances. Methyl spectra of ligatoxin and viscotoxins A3 and B and of phoratoxins A and B are presented in Figures 2 and 3, respectively. As reported previously (Lecomte et al., 1982a), the chemical shifts of resonances stemming from the methyl and its vicinal group, as well as the magnitude of the coupling constant $^3J(CH–CH_3)$ (Campbell et al., 1975), were used to sort signals by amino acid type. The relevant NMR parameters are listed in Tables SI–SIV of the supplementary material (see paragraph at end of paper regarding supplementary material). In all cases, the observed spectroscopic alanine and threonine contents agree with their reported amino acid compositions (Figure 1B). As is the case for crambin (Lecomte et al., 1982a), signals from the other methyl-containing residues are more difficult to identify mainly because the resonances overlap in a narrow region of the spectrum. The toxins, like their homologues, exhibit a complex spectral pattern around 0.9 ppm whose intensity is contributed to by Leu, Val, and Ile resonances.

It was possible in the case of the viscotoxins to match the spectrum provided by the Leu and Ile methyl groups (Figure 2) with the reported compositions (Figure 1B; Tables SI–SIII). On the other hand, for ligatoxin and the phoratoxins the correspondences are tentative: those three protein samples were not fully homogeneous due to the difficulty of fractionating closely homologous proteins, and their spectra reflect this fact. Ligatoxin (Figure 2C) shows several fractional intensity signals, and the phoratoxin A sample, on which the SECSY and decoupling experiments were performed, consists of a 1:1 mixture of the A and B homologues as suggested by a pair of half-integer signals (marked A in Figure 3A) from the methyl groups of Val^{25} in phoratoxin A (Table SIV). A homogeneous sample of phoratoxin B gives a spectrum essentially free of valyl resonances (Figure 3B).

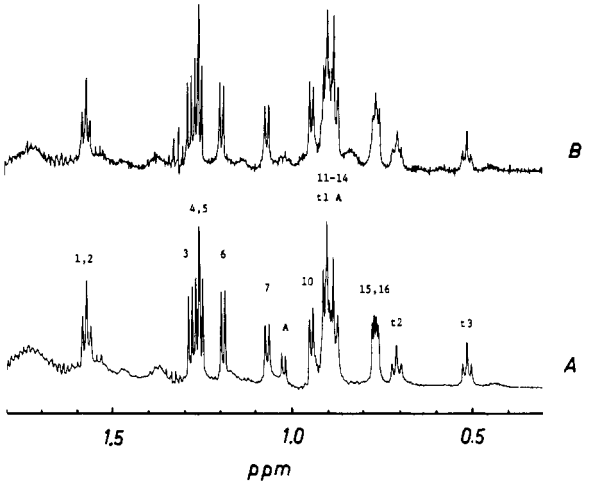

FIGURE 3: ^{1}H NMR spectrum of two phoratoxins at 600 MHz, methyl region. Solvent: ^2H_2O, pH* 6.29, 298 K. (A) Phoratoxin A and B and (B) phoratoxin B. Signals are numbered from low to high field. Except for isoleucyl CH_3^δ triplets (t), all resonances are doublets.

Elsewhere (Lecomte et al., 1982b), we exploited the close structural relationship among members of the thionin group for the assignment of a large number of methyl resonances.[2] A similar analysis was applied to the toxins. Assuming that Ala^{27} decouples at the same frequency in the thionins and in the toxins enabled us to ascribe the resonance marked 1 in the toxins' spectra to that residue. The second Ala signal in the spectrum of viscotoxin B (signal 2 in Figure 2B) must come from Ala^{37} since there are only two such residues in the sequence. Similarly, the second Ala signal in the spectrum of ligatoxin (signal 2 in Figure 2C) must arise from Ala^9. This resonance shares the characteristics of the phoratoxins' Ala^9 (signal 2 in Figure 3). In viscotoxin A3, we assign signal 2 to Ala^{21} because it is close to what was observed for Ala^{21} in the thionins; therefore, signal 6, the remaining alanine, must come from Ala^{15}.

Further comparison with the thionin methyl spectra is not straightforward since only a few residues are common to both sets of proteins (Figure 1B). This is apparent in that spectroscopically they do not exhibit the agreement noticed within the thionin group (Lecomte et al., 1982b) to the extent that methyl protons from the same residue do not resonate within a ~±0.02-ppm range. The correspondences among the toxins' signals are not direct either. As an example, Ile^{12}, Ile^{34}, and Ile^{35} are present in all five toxins but show resonances at different positions in the spectra, which precludes an un-

[2] In our analysis of the α-hordothionin spectrum, a methyl doublet at 1.290 ppm was identified as Thr^{37} (Lecomte et al., 1982b). In view of the recently reported nucleotide sequence of a cDNA encoding for the protein (Ponz et al., 1986), it is now clear that the doublet should be assigned to Thr^{42} (Ozaki et al., 1980).

Table I: Assignment of Methyl Resonances in the Spectra of the Mistletoe Toxins[a]

signal no.	V-A3[b]	V-B[c]	L-A[d]	P-A[e]	P-B[f]
1	Ala^{27}	Ala^{27}	Ala^{27}	Ala^{27}	Ala^{27}
2	Ala^{21}	Ala^{37}	Ala^{9}	Ala^{9}	Ala^{9}
3				Thr^{15}	Thr^{15}
4		Thr^{7}			
5		Thr^{15}			
6	Ala^{15}		Thr^{15}		
7	Thr^{7}				
8					
9					
10	Leu^{29}	Leu^{29}	Leu^{29}	Leu^{29}	Leu^{29}
11	Leu^{29}	Leu^{29}	Leu^{29}	Leu^{29}	Leu^{29}
12	Leu^{18}	Leu^{18}	Leu^{18}		
13	Leu^{18}	Leu^{18}	Leu^{18}		
14					
15					
16					
t1					
t2					
t3					
X				Val^{25}	
t4					Ile^{25}

[a] The numbering refers to the spectra presented in Figures 2 and 3. [b] Viscotoxin A3. [c] Viscotoxin B. [d] Ligatoxin A. [e] Phoratoxin A. [f] Phoratoxin B.

Chart I: Numbering of His and Aromatic Side-Chain Atoms

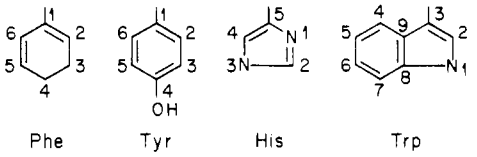

equivocal assignment of their corresponding signals on a comparative basis. This is not surprising considering that aromatic residues shift signals through ring-current effects and play an important part in determining the position of the lines in the spectrum and that the aromatic contents of the toxins differ from that of the thionins and vary among themselves (Figure 1C). With this caveat, it is apparent that the ligatoxin and viscotoxins Ile and Leu methyl spectra (Figure 2) resemble those of the investigated phoratoxins (Figure 3). We tentatively conclude that Ile^{12}, Ile^{34}, Ile^{35}, and Leu^{29} are present in the spectra of these five homologous toxins. Our proposed assignments are summarized in Table I.

Analysis of the Aromatic Spectrum. Among the homologues of crambin, the phoratoxins have the highest aromatic content; their primary structures include Tyr^{13}, Phe^{18}, Trp^{44}, and His^{46} (Figure 1C). The side chains of the aromatic residues are illustrated in Chart I. Figure 4 shows the 300-MHz aromatic spectrum of phoratoxin A plus B at pH* 8.07, 315 K, after ^1H–^2H exchange of the labile N*H* protons. Most conspicuous in this spectrum are the four unsplit peaks at ~7.70, 7.20, 6.95, and 6.70 ppm, numbered 1–4 following the increasing chemical shift scale. Among the aromatic C*H* resonances, only Trp indole H2 and His imidazole H2 and H4 yield virtually unresolved singlets, of area one proton each. Resonance 2 is a deceptive four-proton "singlet" that arises from a casual degeneracy of the Tyr^{13} phenol ring spectrum (discussed below). Peaks 1, 2, and 4 are one proton each and must, therefore, arise from the side chains of Trp^{42} and His^{46}. After the sample was allowed to stand a few hours at 315 K, pH* 8.07, the peak at 7.7 ppm had a decreased intensity implying that the corresponding H atom underwent exchange with solvent deuterium, a behavior that is typical of the His H2 [see, e.g., Markley (1975)]. The singlets can be further characterized on the basis of their acid–base responses as

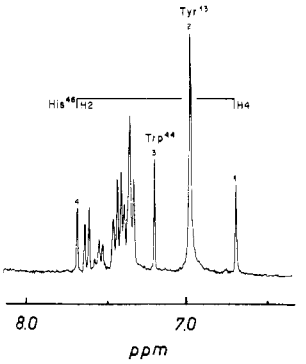

FIGURE 4: ^1H NMR spectrum of phoratoxin A plus B at 300 MHz, aromatic region. Solvent: ^2H_2O, pH* 8.07, 315 K.

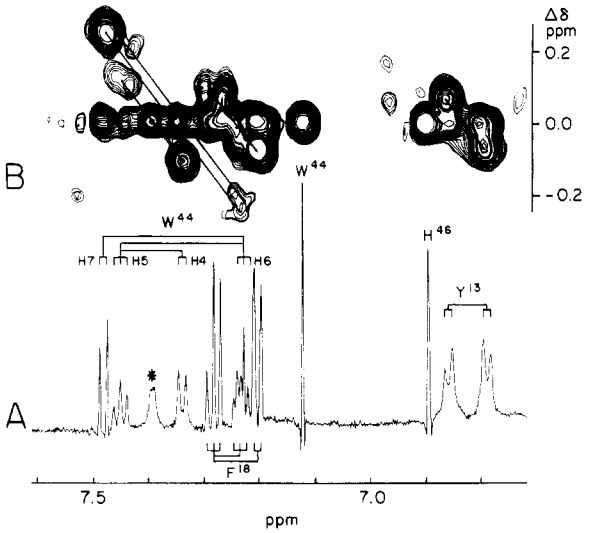

FIGURE 5: ^1H NMR spectrum of phoratoxin A plus B at 600 MHz, aromatic region. Solvent: ^2H_2O, pH* 6.1, 298 K. (A) Reference spectrum and (B) contour plot of the SECSY spectrum. Connectivities are indicated; the conventional one-letter code is used to label amino acid residues.

imidazole groups titrate while indole groups do not. Figure 5A shows, expanded, the 600-MHz aromatic spectrum of phoratoxin A at pH* ~6.0. The singlets detected at 6.7 and 7.7 ppm in the more basic medium (Figure 4) move to ~6.90 and ~8.35 ppm (off scale in Figure 5A), respectively, at pH* 6. The chemical shift of singlet 3 at 7.2 ppm does, in contrast, not vary over the pH* range and is thereby ascribed to the Trp^{44} H2. The pH* dependence of the chemical shift for the three aromatic singlets in phoratoxin B was monitored. It is apparent that the central singlet does not titrate while the two at relatively higher and lower fields titrate with pK_a* ~6.9, corresponding to pK_a ~6.5 once corrected for the ^2H isotope effect (Glasoe & Long, 1960). This experiment leads to assignment of the three singlets as indicated in Figures 4 and 5. Furthermore, the magnitude of the acid/base shifts identifies the His^{46} imidazole H2 and H4 signals individually, which also agrees with the assignments given above on the basis of exchange deuteriation of the C*H*2 site. Both the pK_a* and the overall characteristics (chemical shifts and line widths) of the His^{46} side chain indicate that in the phoratoxins the single C-terminus imidazole group is exposed to the solvent.

It is apparent from comparing the 1-D spectra in Figures 4 and 5A that the degenerate appearance of the Tyr^{13} phenol ring resonances (Figure 4) has been removed on lowering the pH* and temperature to yield, at pH* 6.1, 298 K, a rather broad AA′BB′ pattern well resolved at ~6.83 ppm in the 600-MHz spectrum (Figure 5A). As discussed elsewhere for

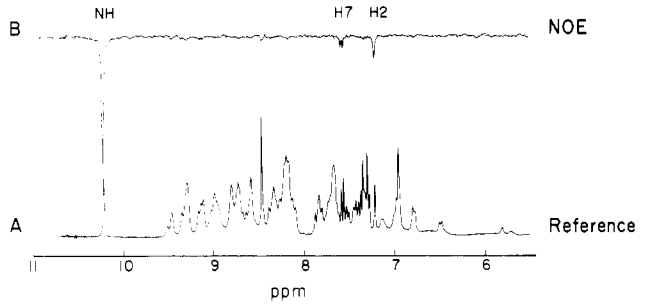

FIGURE 6: Proton Overhauser experiment on phoratoxin B at 300 MHz. Transient response of aromatic proton resonances to selective inversion of the tryptophan indole N*H* magnetization. (A) Reference spectrum and (B) NOE difference spectrum (off-resonance minus Trp irradiated) assigning H2 (singlet) and H7 (doublet) resonances. Both off-resonance (ν_2 = 14.0 ppm) and Trp irradiated (ν_2 = 10.22 ppm) represent the average of 16 000 scans. Sample concentration 8.6 mM in ^1H_2O, pH 5.0, 298 K.

the Tyr^{44} side chain in crambin (Lecomte & Llinás, 1984b), such a fortuitous degeneracy of phenolic H2,6 and H3,5 resonances signifies that the native structure can cause the H2,6 resonance to appear at the same frequency at which the corresponding H3,5 resonance occurs. This is in contrast with the typical "random-coil" pattern where the H2,6 signal is shifted to lower fields from the H3,5 doublet (~7.25 vs. ~6.75 ppm). Thus, in the native phoratoxins, the magnetic environment of the Tyr^{13} side chain is significantly affected by the conformation, yielding Tyr spectral patterns that are reminiscent of those exhibited by the conserved Tyr^{13} ring in the thionins (Lecomte et al., 1982b). Similar nuances of Tyr spectral patterns are observed for the viscotoxins.

Figure 5B shows the corresponding contour plot of the SECSY spectrum at pH* 6.1, 600 MHz. On the basis of their multiplicity, the four Trp^{44} indole signals marked W^{44} can readily be recognized as arising from H4 and H7 (doublets) and H5 and H6 (triplets). Their absolute assignments were derived on the basis of Overhauser experiments in ^1H_2O discussed below. The remaining multicoupled resonances belong to Phe^{18}: one doublet, at 7.20 ppm (H2,6), and two triplets, at 7.28 (H3,5) and 7.22 ppm (H4), in a ratio 2:2:1. The analysis of the phoratoxin aromatic spectrum (Figure 5) was verified by simulation (Lecomte, 1982). It is clear that the Trp indole spectral pattern does not reflect the random-coil ordering, in which the two doublets (H4 and H7) resonate at lower fields than the other three resonances (H2, H5, and H6) (Bundi & Wüthrich, 1979).

The ligatoxin ^{1}H NMR spectrum matches the reported aromatic content (Figure 1C): one each of Tyr, Trp, and His with no Phe residues. These spectra, as well as that of phoratoxin D, have been reported elsewhere (Lecomte, 1982).

Assignment of Trp Indole Resonances. Figure 6A shows the complete low-field spectral region of phoratoxin B recorded in ^1H_2O after being excited with a long, soft pulse to suppress the solvent signal (Redfield, 1978). Because of the unprotected nature of the His^{46} side chain, the imidazole N*H* resonance is expected to be exchange-broadened beyond detectability. Most conspicuous is the presence of a sharp peak at ~10.2 ppm, which is typical of an indole N*H*1 singlet. In phoratoxin B, this signal has to arise from the Trp^{44} side chain. The rest of the N*H* spectrum results from peptidyl amide groups.

The Trp^{44} N*H* transition at 10.2 ppm was selectively inverted with a 50-ms pulse and the magnetization allowed to relax for 400 ms; the NOEs were recorded as a difference spectrum. As shown by Figure 6B, only two signals appear to have been perturbed by the H1 irradiation: the indole doublet at ~7.6 ppm, which hence becomes assigned to the

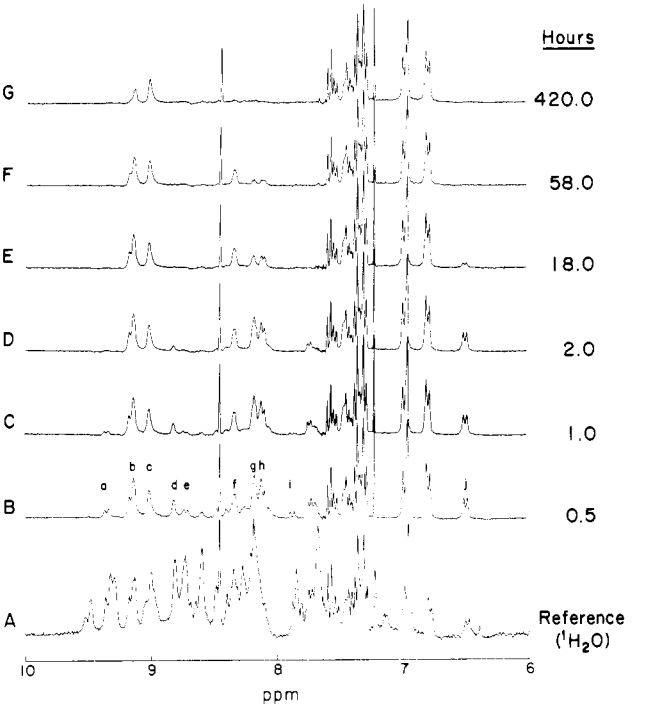

FIGURE 7: Phoratoxin B amide H exchange in ^2H_2O. (A) Reference spectrum recorded for 3.5 mM protein dissolved in ^1H_2O, pH 5.0, 298 K. (B–G) Spectra recorded at the listed times after dissolving the protein in ^2H_2O, 2.5 mM, pH* 5.8, 298 K. The Trp^{44} indole N*H* resonance at 10.22 ppm (Figure 6) is absent from spectrum B due to fast exchange deuteriation. The exchange half-lives for a number of selected N*H* groups were determined: a, 0.68 h; b, 216.61 h; d, 0.84 h; e, 0.38 h; f, 92.42 h; g, 5.98 h; h, 6.30 h; i, 0.45 h; j, 7.07 h. The N*H* group responsible for resonance c is essentially unexchanged within the time period covered by the experiment.

indole H7 proton, and, as expected, the H2 singlet at ~7.2 ppm (Poulsen et al., 1980). This experiment leads to an unambiguous identification of the rest of the Trp^{44} indole proton resonances on the basis of the connectivities determined from the SECSY spectrum (Figure 5).

Structural Micro- and Macrostabilities. The amide proton spectrum of phoratoxin B (Figure 6B) reinforces a picture of a globular conformation endowed with substantial secondary and tertiary structural order (Llinás & Klein, 1975). In order to further characterize the conformation as well as the structural dynamics of phoratoxin B, the protein was dissolved in ^2H_2O, pH* 5.8, and the ^{1}H NMR spectrum recorded as a function of time to monitor the ^{1}H–^{2}H exchange kinetics of N*H* groups (Figure 7B–G). Despite the small size of the protein, about 20 N*H* groups exhibit retarded ^{1}H–^{2}H exchange. Some of these signals (identified by letters a–j in spectrum B) can be readily monitored, as they are relatively well resolved, and exhibit a wide range of exchange rates. Thus, while resonance c arises from an amide that does not exchange with a measurable rate, resonances a, d, e, and i, although exchange retarded, are all relatively short-lived.

One may classify the retarded exchangeable N*H* atoms into three broad categories: very slow ($t_{1/2}$ approximately several days–year; resonances b, c, and f), slow ($t_{1/2}$ approximately several hours; resonances g, h, and j), and fast ($t_{1/2} \lesssim 1$ h; resonances a, b, e, and i). Such a range of exchange kinetics, and the extremely low rate characterizing some of these N*H* groups, suggests that overall the protein structure is compact with a significant dynamic stability. Clearly this feature distinguishes the toxins from the thionin homologues that exchange immediately upon dissolution in ^2H_2O (Lecomte et al., 1982) and even from crambin, whose slow exchange rate

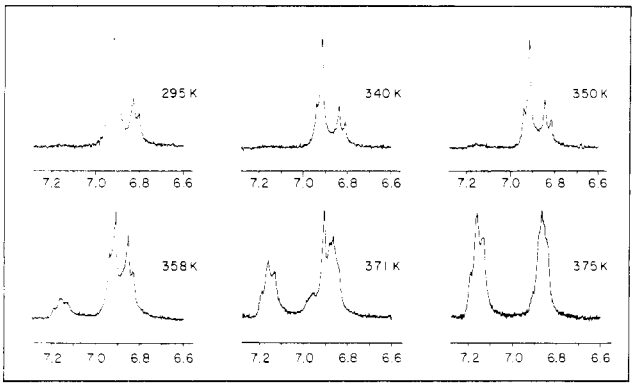

FIGURE 8: ^{1}H NMR tyrosyl spectrum of viscotoxin B at 300 MHz as a function of temperature. Solvent: ^2H_2O, pH* 6.3. Presence of unfolded protein is manifested by the appearance, at high temperatures, of broad resonances at ~6.87 and 7.18 ppm.

(Llinás et al., 1980) has recently been observed to accelerate upon dilution, suggesting it becomes retarded because of self-aggregation (A. Motta and M. Llinás, unpublished observations). The relative lower stability of the thionins vis-ã-vis the mistletoe toxins is somewhat surprising considering that the thionin structure is constrained by an extra cystine bridge linking sites 12 and 30.

H-exchange kinetics provides insights into the microstability of a protein, i.e., the dynamic solvent accessibility of individual peptidyl amide NH and CO sites as determined by the local structural fluctuations and/or cooperative motions (Linderstrøm-Lang, 1958; Hvidt & Nielsen, 1966; Woodward et al., 1982; Englander & Kallenbach, 1983; Tüchsen & Woodward, 1985). A question of interest is the extent to which the microstability of the protein relates to the structural macrostability as measured, e.g., by its thermal unfolding characteristics (Privalov & Tsalkova, 1979). As shown elsewhere (De Marco et al., 1979; Lecomte et al., 1984b; Llinás, 1985), the aromatic tyrosyl spectrum affords a sensitive NMR probe to monitor local thermal unfoldings. Thus, it is expected that with increasing temperature, as the protein expands to eventually assume the unfolded conformation, the ortho and meta phenolic ring doublets of a constrained Tyr ring will shift toward the random-coil AA′XX′ spectrum.

Viscotoxins A3 and B have only two tyrosines, at positions 13 and 43, defining their total aromatic content (Figure 1C). Figure 8 shows the aromatic spectrum of viscotoxin B at various temperatures after exchange of the labile N*H* protons. The aromatic spectrum of viscotoxin B at 295 K clearly shows that one of the tyrosines exhibits the AA′BB′ (Tyr-I) pattern found for Tyr^{13} in the phoratoxins, while the other (Tyr-II) appears as a sharp singlet (AA′A″A‴ pattern)which overlaps, at 295 K, with the lowest field doublet of Tyr-I. The spectral pattern of viscotoxin A3 (not shown) is similar to that of the B homologue. Upon heating viscotoxin B, at pH* 5.75, from 295 to 375 K, the presence of an unfolded species becomes manifest at ~350 K (resonances at ~6.87 and 7.17 ppm), and its relative presence increases upon raising the temperature to 375 K, at which point most of the protein is unfolded. However, gradual lowering of the temperature did not restore the native protein spectrum. In the case of the phoratoxins, a similar experiment shows that the protein native structure is also very stable with respect to reversible thermal unfoldings, although a parallel irreversible denaturation becomes apparent above ~358 K.

Comparison with Other Homologues. As discussed above, the phoratoxins' aromatic Tyr^{13} spectrum exhibits, at 315 K (Figure 4), the singlet-like pattern we have observed in the crambin gramineae homologues (Lecomte et al., 1982b). This behavior indicates that the local characterisitics of the site 13 niche responsible for the quasi-degenerate situation encountered in the phoratoxins are, if not identical, certainly of the same kind as in the thionins, which points to common structural constraints in the two sets of homologues.

In case of the thionins (Lecomte et al., 1982), it appears that a number of amino acids (up to 25% within the set studied, up to 7% pairwise) can be replaced without upsetting the over conformational balance of the protein, in accordance with the proposition of Perutz and co-workers (Perutz et al., 1965). For the mistletoe toxins, however, the degree of primary structure analogy is lesser (39% overall, at least 17% pairwise). Consequently, their ^{1}H NMR spectra show less uniformity, and assigning the resonances to specific residues by matching chemical shifts can be ambiguous. Nonetheless, it is significant that several spectral features are common to the 11 homologues suggesting that definite conformational characteristics are preserved.

It is noteworthy that the duplication of some resonances, attributed in crambin to the presence of two amino acid heterogeneities, is not observed for the phoratoxins even though site 25 of the latter, like site 25 of crambin, is shared by two different residues (Thunberg, 1983). We recall that in crambin (Lecomte et al., 1982a; Lecomte & Llinás, 1984a), the perturbation is the strongest for the residue at site 29 and detectable for many other resonances, among which are those of residue 13 (Phe^{13}). Residue 29 was not identified in the phoratoxin spectrum, but Tyr^{13} gives rise to a single AA′BB′ spin system (Figure 5). As a matter of fact, the two variants yield lines that are perfectly superimposable over the whole spectrum, except, quite naturally, for the signals arising from the residues at site 25, among which a doublet from Val^{25} (A in Figure 3) is readily identified. In crambin, the doubling of the spectrum of a large number of nonproximal groups may, therefore, be related to the heterogeneity at site 22, which results from a Pro → Ser substitution. The nature of the effect is likely to originate from dynamic rather than from conformational differences, for example, the prolyl ring stabilizing (or destabilizing) a backbone dihedral angle.

Recently, Whitlow and Teeter (1985) have reported that α_1-purothionin and crambin exhibit CD spectra in the peptide absorption region that are essentially superimposable with that of viscotoxin A3, providing further support to the assumption of common secondary structure elements. Furthermore, energy minimization calculations that start from the crambin crystallographic coordinates lead to very similar amphipathic tertiary structures for the three proteins (Whitlow & Teeter, 1985).

Conclusions

From our analysis of the ^{1}H NMR spectra of crambin and its homologues, we conclude that in solution these protein have similar globular structures. Crambin itself exhibits a lower homology with the other proteins (45%); however, the fact that three disulfide bridges are conserved throughout the whole set of homologues would appear to impose a most important structural constrain that results in a rather uniform conformational pattern.

Interestingly, as judged from the amide N*H* isotope exchange rates, the mistletoe toxins are dynamically less flexible, despite the extra cystine found in the thionins. Furthermore, in contrast to the gradual thermal transitions observed for crambin (De Marco et al., 1981; Lecomte & Llinás 1984b), both the phoratoxins and viscotoxin B appear to have a rigid structure, not susceptible to significant temperature activation.

Thus, for viscotoxin B, we do not observe any splitting of the Tyr-II singlet up to 378 K, which, in conjunction with the negligible temperature dependence of Tyr-I, indicates that the forces governing the protein conformation arise from rather steep potentials so that it is energetically demanding to thermally excite the protein into higher vibrational levels (Lecomte & Llinás, 1984; Llinás, 1985). The irreversible thermal denaturation that is observed at high temperatures is most likely a consequence of chemical degradation (Ahern & Klibanov, 1985) to be distinguished from the activated, reversible unfoldings (Llinás, 1985).

The structural stability of the mistletoe toxins makes these proteins, in conjunction with the ferrichrome peptides, the bovine pancreatic trypsin inhibitor, and other toxins of animal origin, an interesting system for studying the fundamentals of protein structural dynamics.

Supplementary Material Available

Four tables showing ^{1}H NMR parameters of methyl resonances in the spectra of viscotoxin A3, viscotoxin B, ligatoxin A, and phoratoxins A and B (4 pages). Ordering information is given on any current masthead page.

Registry No. V-A3, 55465-79-7; V-B, 11088-20-3; L-A, 84930-56-3; P-A, 65719-15-5; P-B, 86596-04-5.

References

Ahern, T. J., & Klibanov, A. M. (1985) *Science (Washington, D.C.) 228*, 1280–1284.

Aue, W. P., Bartholdi, E., & Ernst, R. R. (1976) *J. Chem. Phys. 64*, 2229–2246.

Bundi, A., & Wüthrich, K. (1979) *Biopolymers 18*, 285–297.

Campbell, I. D., Dobson, C. M., & Williams, R. J. P. (1975) *Proc. R. Soc. London, A 345*, 23–40.

De Marco, A. (1977) *J. Magn. Reson. 26*, 527–528.

De Marco, A., Menegatti, E., & Guarneri, M. (1979) *Eur. J. Biochem. 102*, 185–194.

De Marco, A., Lecomte, J. T. J., & Llinás, M. (1981) *Eur. J. Biochem. 119*, 483–490.

Englander, S. W., & Kallenbach, N. R. (1983) *Q. Rev. Biophys. 16*, 521–655.

Glasoe, P. K., & Long, F. A. (1960) *J. Phys. Chem. 64*, 188–190.

Hendrickson, W. A., & Teeter, M. (1981) *Nature (London) 290*, 107–113.

Hvidt, A., & Nielsen, S. O. (1966) *Adv. Protein Chem. 21*, 287–386.

Jones, B. L., Lookhart, G. L., Mak, A., & Cooper, D. B. (1982) *J. Hered. 73*, 143–144.

Konopa, J., Woynarowski, J. M., & Lewandowska-Gumieniak, M. (1980) *Hoppe-Seyler's Z. Physiol. Chem. 361*, 1525–1533.

Lecomte, J. T. J. (1982) Ph.D. Dissertation, Carnegie-Mellon University.

Lecomte, J. T. J., & Llinás, M. (1984a) *Biochemistry 23*, 4799–4807.

Lecomte, J. T. J., & Llinás, M. (1984b) *J. Am. Chem. Soc. 106*, 2741–2748.

Lecomte, J. T. J., De Marco, A., & Llinás, M. (1982a) *Biochim. Biophys. Acta 703*, 223–230.

Lecomte, J. T. J., Jones, B. L., & Llinás, M. (1982b) *Biochemistry 21*, 4843–4849.

Linderstrøm-Lang, K. U. (1958) *Proc. Symp. Protein Struct. 9*, 23–24.

Llinás, M. (1985) in *Molecular Dynamics and Protein Structure* (Hermans, J., Ed.) pp 67–72, University of North Carolina, Chapel Hill, NC.

Llinás, M., & Klein, M. P. (1975) *J. Am. Chem. Soc. 97*, 4731–4737.

Llinás, M., De Marco, A., & Lecomte, J. T. J. (1980) *Biochemistry 19*, 1140–1145.

Markley, J. L. (1975) *Acc. Chem. Res. 8*, 70–80.

Mellstrand, S. T. (1974) *Acta Pharm. Suec. 11*, 375–380.

Mellstrand, S. T., & Samuelsson, G. (1973) *Eur. J. Biochem. 32*, 143–147.

Mellstrand, S. T., & Samuelsson, G. (1974a) *Acta Pharm. Suec. 11*, 347–360.

Mellstrand, S. T., & Samuelsson, G. (1974b) *Acta Pharm. Suec. 11*, 367–374.

Nagayama, K., Wüthrich, K., & Ernst, R. R. (1979) *Biochem. Biophys. Res. Commun. 90*, 305–311.

Olson, T., & Samuelsson, G. (1972) *Acta Chem. Scand. 26*, 585–595.

Ozaki, Y., Wada, K., Hase, T., Matsubara, H., Nakamishi, T., & Yoshizumi, H. (1980) *J. Biochem. (Tokyo) 87*, 549–555.

Perutz, M. F., Kendrew, J. C., & Watson, H. M. (1965) *J. Mol. Biol. 13*, 669–678.

Ponz, F., Paz-Ares, J., Hernández-Lucas, C., Garcia-Olmedo, F., & Carbonero, P. (1986) *Eur. J. Biochem. 156*, 131–135.

Poulsen, F. M., Hoch, J. C., & Dobson, C. M. (1980) *Biochemistry 19*, 2597–2607.

Privalov, P. L., & Tsalkova, T. N. (1979) *Nature (London) 280*, 693–696.

Redfield, A. G. (1978) *Methods Enzymol. 49*, 253–270.

Redman, D. G., & Fisher, N. J. (1969) *J. Sci. Food Agric. 20*, 1110–1111.

Rosell, S., & Samuelsson, G. (1966) *Toxicon 4*, 107–110.

Samuelsson, G. (1961) *Sven. Farm. Tidskr. 65*, 481–494.

Samuelsson, G. (1966) *Acta Chem. Scand. 20*, 1546–1554.

Samuelsson, G., & Ekblad, S. (1967) *Acta Chem. Scand. 21*, 849–856.

Samuelsson, G., & Pettersson, B. M. (1970) *Acta Chem. Scand. 24*, 2751–2756.

Samuelsson, G., & Pettersson, B. M. (1971a) *Eur. J. Biochem. 21*, 86–89.

Samuelsson, G., & Pettersson, B. M. (1971b) *Acta Chem. Scand. 25*, 2048–2054.

Samuelsson, G., Seger, L., & Olson, T. (1968) *Acta Chem. Scand. 22*, 2624–2642.

Selawry, O. S., Vester, F., Mai, W., & Schwartz, M. R. (1961) *Hoppe-Seyler's Z. Physiol. Chem. 324*, 262–281.

Teeter, M. M., Mazer, J. A., & L'Italien, J. J. (*1981*) *Biochemistry 20*, 5437–5443.

Thunberg, E. (1983) *Acta Pharm. Suec. 20*, 115–122.

Thunberg, E., & Samuelsson, G. (1982a) *Acta Pharm. Suec. 19*, 285–292.

Thunberg, E., & Samuelsson, G. (1982b) *Acta Pharm. Suec. 19*, 447–456.

Tüchsen, E., & Woodward, C. (1985) *J. Mol. Biol. 185*, 421–430.

Van Etten, C. H., Nielsen, H. C., & Peters, J. E. (1965) *Phytochemistry 4*, 467–473.

Van Geet, A. L. (1970) *Anal. Chem. 42*, 679–680.

Whitlow, M., & Teeter, M. M. (1985) *J. Biomol. Struct. Dyn.* 2, 831–848.
Winterfeld, K., & Bijl, L. H. (1948) *Justus Liebigs Ann. Chem. 516*, 107–114.
Woodward, C., Simon, I., & Tüchsen, E. (1982) *Mol. Cell. Biochem. 48*, 135–160.
Woynarowski, J. M., & Konopa, J. (1980) *Hoppe-Seyler's Z. Physiol. Chem. 362*, 1535–1545.

Potato Tuber Cyclic-Nucleotide Phosphodiesterase: Selective Inactivation of Activity vs. Nucleoside Cyclic 3′,5′-Phosphates and Properties of the Native and Selectively Inactivated Enzyme†

Małgorzata Zan-Kowalczewska, Jarosław M. Ciešla, Halina Sierakowska, and David Shugar*
Institute of Biochemistry and Biophysics, Polish Academy of Sciences, Rakowiecka 36, 02-532 Warszawa, Poland
Received July 9, 1986; Revised Manuscript Received October 2, 1986

ABSTRACT: Exposure of higher plant (potato tuber) cyclic-nucleotide phosphodiesterase (cPDase, EC 3.1.4) to alkaline pH at 45 °C leads to irreversible selective loss of activity vs. 3′,5′-cAMP with full maintenance of activity vs. 2′,3′-cAMP. There is also loss of most (~80%) of the activity vs. the *p*-nitrophenyl esters of pT and Tp but retention of full activity vs. *p*-nitrophenyl phenylphosphonate and bis(*p*-nitrophenyl) phosphate. The phosphonate ester, proposed as a specific substrate for 5′-nucleotide PDases [Kelly, S. J., Dardinger, D. E., & Butler, L. G. (1975) *Biochemistry 14*, 4983–4988], is now seen to be an excellent substrate for the activity of higher plant cPDase vs. nucleoside cyclic 2′,3′-phosphates. And, in fact, the phosphonate substrate competitively inhibits hydrolysis of 2′,3′-cAMP (K_i ~ 0.3 mM) and vice versa (K_i ~ 0.05 mM). Hydrolysis of the phosphonate ester is also inhibited by 3′,5′-cAMP, but with a K_i 1–2 orders of magnitude higher. The potato enzyme, previously shown to be a tetramer, may be reversibly dissociated to the monomer, with full retention of all activities. Selective inactivation proceeds at the level of the monomer, following which reassociation to the tetramer is minimal and not accompanied by recovery of activity vs. 3′,5′-cAMP. Isoelectric focusing resolves the enzyme into five isozyme fractions, with p*I* values ranging from 6.8 to 8.1. All five fractions exhibit identical properties as regards molecular weight and substrate specifities both prior to and following selective inactivation. The foregoing findings readily account for conflicting reports on the properties of higher plant cyclic-nucleotide phosphodiesterases. Attention is drawn to some similarities with the nonconventional mammalian cyclic-nucleotide phosphodiesterase reported by Helfman and Kuo [Helfman, D. M., & Kuo, J. F. (1982) *J. Biol. Chem. 257*, 1044–1047].

Cyclic-nucleotide phosphodiesterase (cPDase)[1] has been isolated and variously characterized from a variety of higher plants (Brown & Newton, 1981). Unlike the corresponding enzymes from mammalian cells, with one important exception (Helfman & Kuo, 1982; see below), the plant enzymes exhibit broad specificity and hydrolyze both cyclic 2′,3′- and cyclic 3′,5′-phosphates of nucleosides (Vandepeute et al., 1973; Ashton et al., 1975; Shinshi et al., 1976; Zan-Kowalczewska et al., 1984). Rare exceptions include the enzyme from beans (Brown et al., 1977), reported inactive toward nucleoside cyclic 2′,3′-phosphates, and that from cultured tobacco cells, with very low activity vs. nucleoside cyclic 3′,5′-phosphates (Matsuzaki & Hashimoto, 1981), in disagreement with another report (Shinshi et al., 1976). This confusing situation has rendered difficult attempts to clarify the functional role of plant cPDases, the more so in that almost all preparations contain nucleotide pyrophosphatase activity (Zan-Kowalczewska et al., 1984).

We have recently succeeded in purifying potato tuber cPDase to near homogeneity, with only residual (~0.5%) pyrophosphatase activity (Zan-Kowalczewska et al., 1984). Apart from previously described activities, the purified enzyme also cleaved aryl esters of nucleoside 3′- and 5′-phosphates, nucleoside 5′-di- and 5′-triphosphates, aryl phosphonates, and the 2′,3′-cGMP terminal residue of a fragment of TMV RNA (Zan-Kowalczewska et al., 1984).

During the course of further attempts to resolve the nature of the activity of this enzyme against such a multitude of substrates, it was observed that storage of the purified enzyme at 4 °C at pH 7.5 led to selective loss of activity against nucleoside cyclic 3′,5′-phosphates, without affecting activity vs. nucleoside cyclic 2′,3′-phosphates. This phenomenon has now been further examined, with results that undoubtedly contribute to a better understanding of the substrate specificity of this ubiquitous enzyme.

† This investigation profited from the support of the Polish Academy of Sciences (Project CPBR 3.13) and the Polish Cancer Research Program (Project CPBR 11.5).

[1] Abbreviations: PDase, phosphodiesterase; cPDase, cyclic-nucleotide phosphodiesterase; SDS, sodium dodecyl sulfate; SDS–PAGE, SDS–polyacrylamide gel electrophoresis; nitrophenyl-pT, thymidine 5′-(*p*-nitrophenyl phosphate); Tp-nitrophenyl, thymidine 3′-(*p*-nitrophenyl phosphate); BIS, bis(*p*-nitrophenyl) phosphate; AS-BI-naphthol, 6-bromo-2-hydroxy-3-naphthoic acid 2-methoxyanilide; AS-BI-naphthyl-pT, thymidine 5′-(AS-BI-naphthyl phosphate); NEM, *N*-ethylmaleimide; PMSF, phenylmethanesulfonyl fluoride; IEF, isoelectrofocusing; PEI, poly(ethylenimine); Tris, tris(hydroxymethyl)aminomethane; EDTA, ethylenediaminetetraacetic acid.

0006-2960/87/0426-1194$01.50/0